JACS
JOURNAL OF THE AMERICAN CHEMICAL SOCIETY
Article
Cite This: J. Am. Chem. Soc. 2018, 140, 10909−10914
pubs.acs.org/JACS

Molecular Basis for the Final Oxidative Rearrangement Steps in Chartreusin Biosynthesis

Yi Shuang Wang,[†,Δ] Bo Zhang,[†,Δ] Jiapeng Zhu,[*,‡] Cheng Long Yang,[†] Yu Guo,[#] Cheng Li Liu,[†] Fang Liu,[∥] Huiqin Huang,[§] Suwen Zhao,[#] Yong Liang,[∥] Rui Hua Jiao,[†] Ren Xiang Tan,[*,†,‡] and Hui Ming Ge[*,†]

[†]State Key Laboratory of Pharmaceutical Biotechnology, Institute of Functional Biomolecules, School of Life Sciences, Nanjing University, Nanjing 210023, China

[‡]State Key Laboratory Cultivation Base for TCM Quality and Efficacy, School of Medicine and Life Sciences, Nanjing University of Chinese Medicine, Nanjing 210023, China

[#]iHuman Institute, Shanghai Tech University, Shanghai 201210, China

[§]Institute of Tropical Biosciences and Biotechnology, Key Laboratory of Biology and Genetic Resources of Tropical Crops of Ministry of Agriculture, Chinese Academy of Tropical Agricultural Sciences, Haikou 571101, China

[∥]State Key Laboratory of Coordination Chemistry, Jiangsu Key Laboratory of Advanced Organic Materials, School of Chemistry and Chemical Engineering, Nanjing University, Nanjing 210023, China

Supporting Information

ABSTRACT: Oxidative rearrangements play key roles in introducing structural complexity and biological activities of natural products biosynthesized by type II polyketide synthases (PKSs). Chartreusin (**1**) is a potent antitumor polyketide that contains a unique rearranged pentacyclic aromatic bilactone aglycone derived from a type II PKS. Herein, we report an unprecedented dioxygenase, ChaP, that catalyzes the final α-pyrone ring formation in **1** biosynthesis using flavin-activated oxygen as an oxidant. The X-ray crystal structures of ChaP and two homologues, docking studies, and site-directed mutagenesis provided insights into the molecular basis of the oxidative rearrangement that involves two successive C−C bond cleavage steps followed by lactonization. ChaP is the first example of a dioxygenase that requires a flavin-activated oxygen as a substrate despite lacking flavin binding sites, and represents a new class in the vicinal oxygen chelate enzyme superfamily.

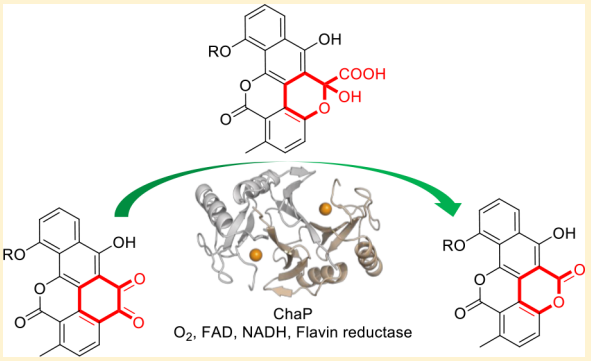

INTRODUCTION

Linear and angular aromatic polyketides biosynthesized by bacterial type II polyketide synthases (PKSs) can be morphed into structurally diverse natural products by an assortment of redox enzymes. These oxidative rearrangements dramatically expand the structural complexity and increase the biological activities of aromatic polyketides. Examples include the biosynthesis of the γ-pyrone ring in xantholipin,[1] dihydropyridine ring in jadomycin,[2] spiro-rings in fredericamycin[3] and griseorhodin,[4] cyclopentadiene ring in kinamycin,[5] and α-pyrone ring in chartreusin,[6] as shown in Figure 1. Considering the key role of oxidation in generating complex natural products,[7] the discovery of novel multifunctional oxidase from nature is of great interest not only to find new natural catalysts but also to develop new methodology in the application of organic and medicinal chemistry.

Chartreusin (**1**), which was originally isolated from *Streptomyces chartreusis* during screening of antibacterial agents against *Mycobacterium tuberculosis*, consists of a structurally unique pentacyclic aromatic bilactone aglycone and a disaccharide (Figure 1).[8] Compound **1** is a potent DNA-binding antitumor agent via radical-mediated single-strand DNA break, and inspired the development of IST-622, a novel semisynthetic derivative of **1** showing promising anticancer activity in a phase II clinical study.[9] The *cha* gene cluster for the biosynthesis of **1** was identified from *S. chartreusis* HKI-249 revealing a type II PKS biosynthetic origin.[6] However, its detailed biosynthetic steps to construct the unusual aglycone has been a subject of much speculation. It was proposed that a linear anthracycline aromatic polyketide **2** derived from 10 malonyl-CoA and an *S*-adenosyl methionine was a putative biosynthetic intermediate (Figure 2A). Then, a Baeyer−Villiger oxidation followed by ring rearrangement and lactonization is thought to take place and give the pentacyclic *o*-benzoquinone compound **3**. Finally, an unprecedented oxidative rearrangement, which was most likely catalyzed by a dioxygenase ChaP and other additional enzymes,[6,7] is

Received: June 27, 2018
Published: August 1, 2018

DOI: 10.1021/jacs.8b06623
J. Am. Chem. Soc. 2018, 140, 10909−10914

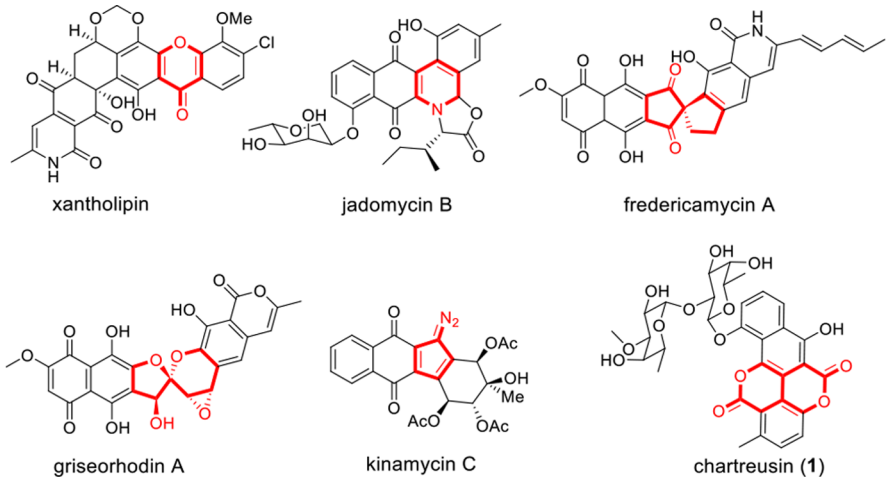

Figure 1. Examples of natural products synthesized by type II PKSs where oxidative rearrangement (highlighted in red) play a key role in generating structural complexity.

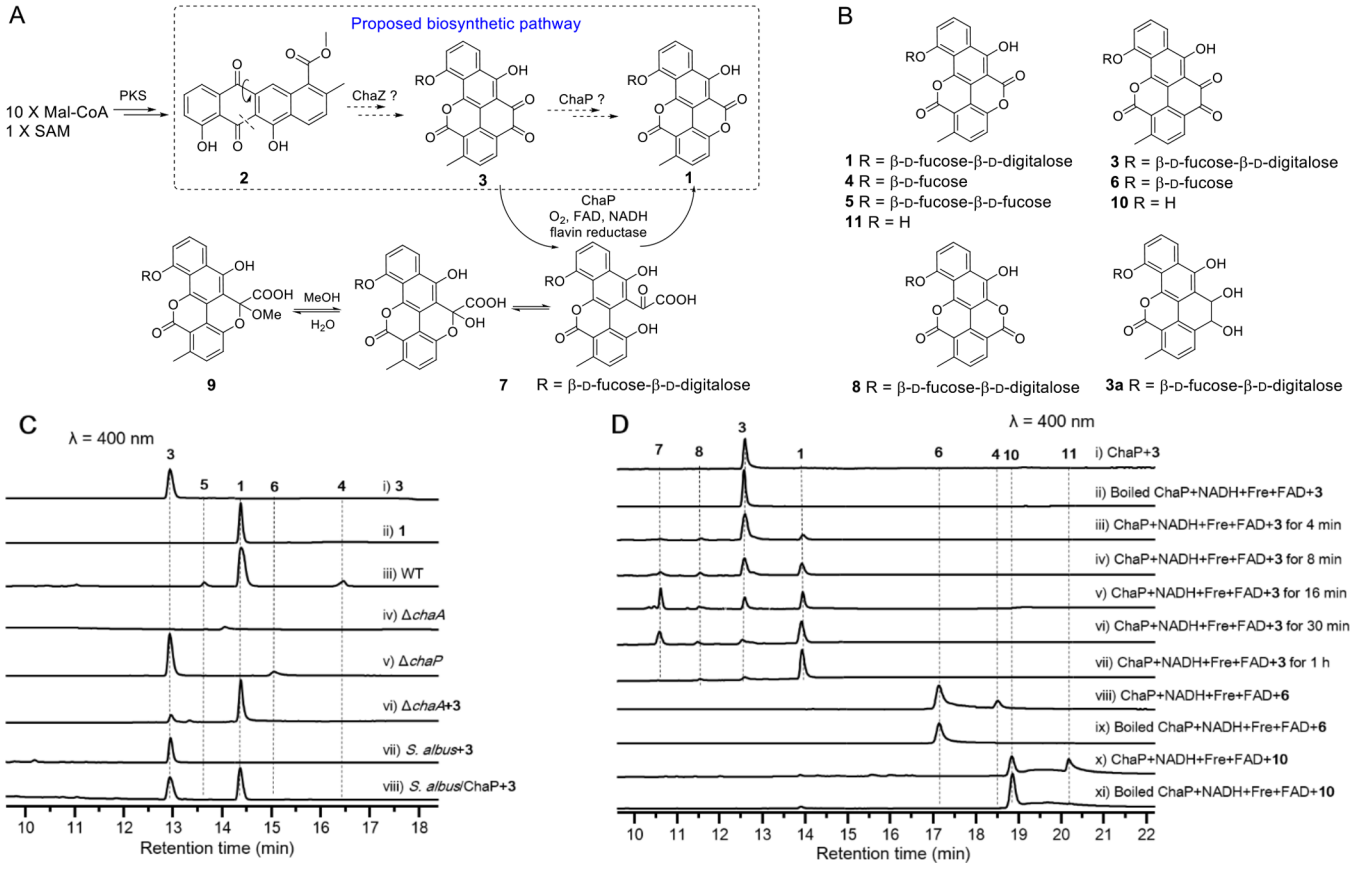

Figure 2. Biosynthesis of chartreusin (**1**). (A) Biosynthetic pathway for **1**. (B) Compounds isolated from WT, mutant strains, and enzymatic and chemical reactions. (C) HPLC analysis of metabolic extracts from WT, mutant, and complementary strains. (D) *In vitro* biochemical reactions catalyzed by ChaP.

proposed to yield **1** (Figure 2A). Here, we demonstrate that ChaP, a rather small enzyme consisting of only 130 amino acid residues, catalyzes the final oxidative rearrangement steps from **3** to **1** through an intermediate **7** in the presence of flavin-activated oxygen (Figure 2A). The crystal structures of ChaP and two homologous enzymes were determined at resolutions of 1.6−2.0 Å. In addition, docking studies and site-directed mutagenesis revealed the molecular basis for this unusual oxidative rearrangement.

RESULTS AND DISCUSSION

Identification of Chartreusin Biosynthetic Gene Cluster from *S. chartreusis* NA02069. The initial antibacterial screening from our strain collection led to the isolation of **1**[8] together with its monosaccharide (**4**)[10] and 9′-desmethyl (**5**)[11] derivatives from *S. chartreusis* NA02069 (Figure 2C-iii, and Supporting Information Tables S4, S7, and S8).[12] The high titer (~1.0 g/L) of **1** provided an

DOI: 10.1021/jacs.8b06623
J. Am. Chem. Soc. 2018, 140, 10909−10914

opportunity to reinvestigate the enigmatic steps in the biosynthesis of **1**, as biosynthetic intermediates from mutant strains may accumulate in sufficient quantities for elucidation of the biosynthetic pathway. Therefore, the genome of the producing strain NA02069 was sequenced by a combination of PacBio and NGS and assembled to a complete linear chromosome. The putative chartreusin biosynthetic gene cluster (*cha*) was then identified and showed the same gene organization and a high degree of identity (>95%) to that in *S. chartreusis* HKI-249 (Table S3).[6] Inactivation of the KSα-encoding gene *chaA* completely abolished the production of **1**, as well as **4** and **5** (Figure 2C-iv), confirming the link between the *cha* cluster and the biosynthesis of **1**.

***In Vivo* Characterization of ChaP.** To examine the role of ChaP, we knocked out the *chaP* gene in wild-type (WT) *S. chartreusis* NA02069. The resulting Δ*chaP* mutant strain abolished the production of **1**, **4**, and **5** but accumulated two new compounds **3** and **6** (Figure 2C-v). We then fermented the Δ*chaP* mutant strain in large scale and obtained sufficient quantities of both compounds for characterization. Compound **3** was shown to have a molecular formula of $C_{33}H_{32}O_{14}$ by its HRESIMS ion at *m*/*z* 675.1696 ([M+Na]$^+$). The NMR spectra of **3** was comparable to those of **1**, except for the presence of an additional carbonyl carbon signal at δ_C 182.6 (C-15), which showed an HMBC correlation with a downfield aromatic proton signal at δ_H 8.39 (H-17) (Table S5), suggesting this carbonyl carbon connected at C-16. To further disclose its structure, **3** was reduced with $NaBH_4$ to afford a diol derivative **3a** with a molecular formula of $C_{33}H_{36}O_{14}$ (*m*/*z* 679.1992, [M+Na]$^+$). The HMBC correlations of H-14 (δ_H 5.31, d, *J* = 6.0 Hz) with C-4 (δ_C 115.1), C-6 (δ_C 147.6), and C-16 (δ_C 134.4), and of H-15 (δ_H 4.82, d, *J* = 6.0 Hz) with C-3 (δ_C 132.7), C-5 (δ_C 113.7), and C-17 (δ_C 134.0) established the structure of **3a** (Figure 2B, Table S6). Thus, **3** is indeed the expected *o*-benzoquinone intermediate as shown in Figure 2A. Compound **6** was determined as the monosaccharide derivative of **3** (Figure 2B, Table S9). When **3** was supplied to the Δ*chaA* strain, production of **1** was restored (Figure 2C-vii), thereby verifying **3** is an on-pathway biosynthetic intermediate. On the other hand, the conversion of **3** to **1** in Δ*chaA* background cannot exclude the possibility that other downstream enzymes encoded in *cha* gene cluster may also be involved in the biotransformation. Thus, we cloned *chaP* gene into a *Streptomyces* integrative vector pSET152 under the control of *KasO** promoter and transformed the resultant plasmid into *S. albus* J1074. Upon feeding of **3** into *S. albus* J1074 expressing *chaP* gene, around half conversion of **3** to **1** was obtained after 12 h of culture (Figure 2C-viii), indicating ChaP is sufficient for catalyzing this oxidative rearrangement.

Biochemical Characterization of ChaP and Identification of a Key Intermediate. The successful biotransformation of **3** to **1** encouraged us to dissect this unusual reaction in detail. We thus overproduced and purified ChaP as a colorless protein from *Escherichia coli* BL21(DE3) (Figure S2). Unfortunately, no activity was observed when **3** was incubated with ChaP (Figure 2D-i), in spite of our exhaustive efforts.

We thus re-analyzed the nature of ChaP. Notably, ChaP does not have high sequence identity (>30%) to any characterized proteins, but it belongs to the vicinal oxygen chelate (VOC) enzyme superfamily (Figure S3).[13] Members of this family include glyoxalase I, the fosfomycin resistance proteins, two-substrate α-keto acid-dependent oxygenases, and the catechol 2,3-dioxygenases,[13] the latter of which catalyze the non-heme iron-dependent oxidative cleavage of C−C bond adjacent to the vicinal hydroxyl groups in catechol using O_2 as oxidant (Figure S4).[14,15] Most likely, ChaP catalyzes a catechol 2,3-dioxygenase-like reaction to cleave the C−C bond in *o*-benzoquinone. However, these dioxygenases require catechol to coordinate with iron center, and there is no precedence that *o*-benzoquinone, which has two electrons less than that of catechol, can be accepted as substrate. We thus speculated that (i) the *o*-benzoquinone group in **3** must first be reduced by a ketoreductase-like enzyme to afford catechol-type compound as the substrate, or, (ii) the two-electron rich O_2^{2-} or its equivalent serves as the oxidant instead of regular O_2.

The first possibility can be excluded as no additional ketoreductase is required in the biotransformation from **3** to **1** as mentioned before. For the second hypothesis, the most common O_2^{2-} equivalent in secondary metabolism is 4a-flavin hydroperoxide (Fl-4a-OOH), which is derived from two successive one-electron transfers from FlH_2 to oxygen.[16] We thus attempted to incubate **3** with ChaP in the presence of NADH, FAD, and flavin reductase (Fre) from *E. coli*,[17] followed by LC-MS analysis. Surprisingly, after 30 min of incubation the production of **1** was observed along with two minor compounds **7** (*m*/*z* 709.1739 [M+Na]$^+$) and **8** (*m*/*z* 663.1675 [M+Na]$^+$) (Figure 2D-vi). In contrast, no reaction occurred when boiled ChaP was used (Figure 2D-ii). To obtain sufficient **7** and **8** for structure elucidation, a large-scale enzymatic reaction was performed. Compound **8** was isolated and characterized as a shunt metabolite (Figure 2B and Table S10). Purification of **7** was challenging as it converted to **1** spontaneously. However, during purification, a methyl derivative **9** with a molecular formula of $C_{33}H_{34}O_{16}$ (*m*/*z* 723.1893 [M+Na]$^+$) was precipitated from the methanol solution of **7**. Complete 1D and 2D NMR of **9** indicated the structure of **9** is similar to that of **1**. Additional methoxyl and carboxylic acid groups at C-2 were observed by a key HMBC correlation of *O*-methoxyl group (δ_H 3.24) with a sp^3-hybridized quaternary carbon C-2 (δ_C 100.6) as well as a characteristic chemical shift (δ_C 169.3) for a carboxylic group. The structure of **9** was further reinforced by comparison of experimental and calculated ^{13}C NMR chemical shifts (Table S11). The structure of **7** is thus proposed to have a hemiketal group at C-2 (Figure 2A).

The identification of **7** raised the question if it is a biosynthetic intermediate from **3** to **1**. We thus conducted a time-course analysis for the ChaP-catalyzed reaction. The production of **7** increased at early time point, which finally converted to **1** when substrate **3** was consumed (Figure 2D-iii−vii). As **7** can also be converted to **1** spontaneously, we further measured the effect of ChaP concentration on the rate of reaction when **9** was used as substrate, which can converted to **7** in aqueous solution. The production of **1** increased with increasing the concentrations of ChaP (Figure S6). Moreover, the conversion of **9** to **1** required the presence of all co-enzymes and cofactors, as omitting any one of them led to dramatically decrease conversion rates (Figure S6). Taken together, these data firmly establish that ChaP is responsible for two successive steps in conversion of **3** to **1** through the intermediate **7**.

Next, we investigated the effect of various co-enzymes and cofactors for ChaP activity. Four flavin reductases (Figure S7) cloned from the genome of *S. chartreusis* NA02069 were overproduced and purified as bright yellow proteins, suggesting all of them carry flavin cofactors FAD or FMN. The identities

DOI: 10.1021/jacs.8b06623
J. Am. Chem. Soc. 2018, 140, 10909−10914

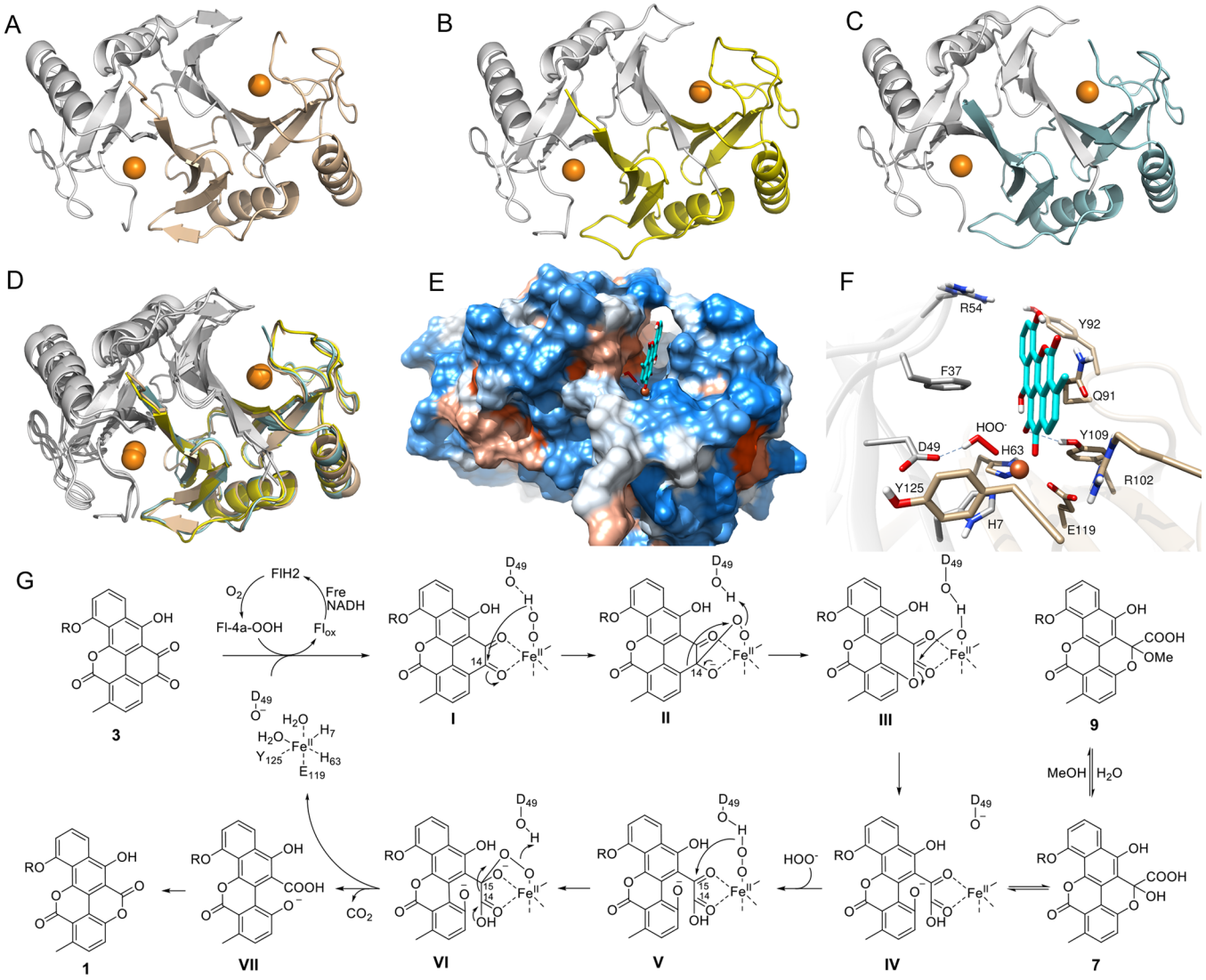

Figure 3. Structures of ChaP and its homologous enzymes and proposed catalytic mechanism. The dimeric structure of ChaP (PDB: 6A4Z) (A), ChaP-H1 (PDB: 6AS2) (B), and ChaP-H2 (PDB: 6A4X) (C). (D) Superimposed image of ChaP (wheat), and its homologues ChaP-H1 (yellow) and ChaP-H2 (aquamarine) and their symmetric monomer was marked as light gray. (E) Colored surface of ChaP and the putative substrate position by docking. The molecular surface was colored by amino acid hydrophobicity according to the Kyte−Doolittle scale: the hydrophobicity scale from lowest to highest was colored blue to orange to red with zero hydrophobicity colored as white. (F) Amino acid residues in ChaP that form the active site. Residues from two monomers are colored in gold and silver, respectively. (G) Proposed mechanism for ChaP-catalyzed reaction.

of these cofactors were determined by comparison of authentic FAD or FMN standards by LC/MS analysis (Figure S8). Comparable amounts of **1** were produced by replacing Fre with either of these four flavin reductases (Figure S9). No products were observed when either Fre or NADH was omitted from reaction system (Figure S9). The conversion rate of **1** was significantly decreased when NADH was substituted with NADPH (Figure S9). Moreover, the activity of ChaP was almost lost when metal ion in ChaP was removed by EDTA, or replaced with other divalent cations such as Co^{2+}, Mg^{2+}, Cu^{2+}, and Mn^{2+}, or with Fe^{3+}, but can be rescued by Fe^{2+} (Figure S10). It is notable that no activity was observed when ChaP was incubated with **3** in the presence of H_2O_2 (Figure S9), suggesting the hydroperoxide anion may require flavin cofactor for delivery. In addition, ChaP can accept aglycone **6** and monosaccharide derivative **10** as substrates to produce **4** and **11**, respectively (Figure 2D, viii−xi).

***In Vitro* Characterization of ChaP Homologues.** Homologues of *chaP* gene are widely distributed in bacterial genomes and are mainly embedded in primary biosynthetic pathways (Tables S15−S22). A phylogenetic tree was constructed to include ChaP, its homologues, and other enzymes in the VOC superfamily. ChaP and its homologues were found to fall into a separate clade from other enzymes in the VOC family (Figure S11). As none of these homologous proteins is functionally characterized, we were curious if they catalyze similar reaction. Thus, eight ChaP homologous enzymes (designated as ChaP-H1 to ChaP-H8, Figure S12) with amino acid sequence identities ranging from 65% to 30% were overproduced to homogeneity (Figure S2). Intriguingly, five homologues (ChaP-H1−ChaP-H5) can efficiently convert **3**, **6**, and **10** to **1**, **4**, and **11**, respectively, with comparable conversion rates to that of ChaP; whereas three of them were inactive (Figures S13−S15). It is uncertain at this stage why

DOI: 10.1021/jacs.8b06623
J. Am. Chem. Soc. 2018, 140, 10909−10914

these homologous enzymes showed activities toward **3**, as no *cha* or similar gene clusters are encoded in their genomes. Nonetheless, it can be speculated that these enzymes take part in the degradation of *o*-benzoquinone-type compounds from the environment.

Crystal Structures of ChaP and Two Homologues. To further investigate the mechanistic details of the unusual reaction, the structures of ChaP and two homologous proteins ChaP-H1 from *Rhodococcus phenolicus* and ChaP-H2 from *Streptomyces curacoi* were solved at 1.70, 2.00, and 1.63 Å resolution, respectively (Table S23). ChaP-H1 and ChaP-H2 share 65% and 61% amino acid sequence identity with ChaP, respectively. Analysis of the crystal structures revealed a symmetric homodimer with each monomer featuring two similar $\beta\alpha\beta\beta$ motifs (Figure 3A–C). These enzymes are structurally highly similar to each other with r.m.s. deviations of 0.8–1.0 Å (Figure 3D). The location of two narrow symmetric active pockets, which likely accommodate the plate-shaped substrate, is defined by the presence of two Fe^{II} ion binding sites in the interface of the two monomers (Figure 3). Fe^{II} ion is coordinated by one tyrosine residue (Y125), one glutamate residue (E119), a pair of histidine residues (H7 and H63), and two water molecules with an average distance of 2.23 Å (Figure S17). Moreover, one of the histidine residues (H7) is from the other monomer.

Docking Study and Site-Directed Mutagenesis of ChaP. Three-dimensional structure searching using the Dali server[18] revealed that ChaP homodimer shares similarity to BphC (PDB: 1KW8) from *Pseudomonas* sp. in terms of Fe^{II} binding sites with r.m.s. deviations of 2.3 Å (Figure S18),[19] albeit extremely low sequence identity (<5%). BphC is a well-characterized 2,3-catechol dioxygenase in the VOC enzyme family, which catalyze the non-heme Fe^{II}-dependent oxidative cleavage of catechols to 2-hydroxymuconaldehyde products.[19] Docking of the ChaP with **10** and hydroperoxide anion (HOO^-) was conducted by the Induced Fit Docking workflow.[20] The final docking poses were selected using BphC-substrate-NO (nitric oxide) complex structure (PDB: 1KW8) as reference. As shown in Figure 3F and Figure S19, the substrate coordinated with Fe^{II} through *o*-quinone group in a narrow groove, and was clamped by Q91, Y92, Y109, and R102 from one side, and F37 and R54 from another side; the HOO^- was surrounded by D49, F37, and Y125. The big aromatic π-electron system of the substrate has strong T-shaped $\pi-\pi$, amide$-\pi$, $\sigma-\pi$, and cation$-\pi$ interactions with F37, Y109, Q91, and R102. Importantly, two hydrogen bonds were observed between D49 and HOO^-, and Y109 and O-14 of substrate **10**.

To investigate the individual role of the above putative active residues, systematic site-directed mutagenesis of ChaP was performed. Consistent with the observed hydrogen bonds in docking study, both D49A and Y109A mutants showed 9-fold and ~33-fold decreases in conversion rates, respectively. The Q91A mutant retained the activity, whereas, the Q91L resulted in a 7-fold decreased activity putatively by steric hindrance. Moreover, the Q91E resulted in ~40% loss in conversion rate, suggesting the neutral charge is important for its activity. Other mutations including Y92F, Y125A, Y125F, R102L, F37A, and R54L maintained substantial activity, indicating these residues may only have structural roles or have week interaction with substrate (Figure S20).

Proposed Mechanism of ChaP. Taking all these data together, we propose a plausible mechanism for the ChaP-catalyzed oxidative rearrangement mechanism (Figure 3G). After coordination of the *o*-benzoquinone group with Fe^{II}, the flavin-activated hydroperoxide anion (HOO^-) enters the active site and binds to Fe^{II}. The neighboring D49 stabilizes HOO^- by forming a hydrogen bond and initiates the reaction through deprotonation. The peroxide anion performs a nucleophilic attack at C-14, leading to the formation of intermediate **II**. Similar to the catalytic mechanism found in 2,3-catechol dioxygenase,[14,15] a Criegee rearrangement will take place to yield seven-membered lactone intermediate **III**, followed by a subsequent hydrolysis to afford α-keto acid **IV**. Once the formed α-keto acid diffuses out of the active site, it will undergo a spontaneous ring closure to give the hemiketal compound **7**, which can be further transformed to **9** in the presence of methanol. On the other hand, a second molecule of flavin-activated HOO^- can rebound to Fe^{II} of **IV**, leading to the formation of intermediate **V**. The peroxide anion can then attack C-15 to arrive at **VI** followed by C-14–C-15 cleavage to form **VII** with the release of a molecular of CO_2. **VII** can undergo a spontaneous lactonization to give final product **1**.

CONCLUSION

We have identified the key oxidative rearrangement steps for installing the final α-pyrone ring in the biosynthesis of **1**. Our present data indicated that ChaP is a novel bifunctional enzyme, which not only catalyzes the oxidative cleavage of C–C bond adjacent to *o*-quinone to afford intermediate **7** via a "2,3-catechol dioxygenase"-like mechanism, but also mediates an oxidative decarboxylation to finally generate the α-pyrone moiety. It is unprecedented that ChaP and its homologous enzymes accept *o*-benzoquinone and flavin-activated oxygen (O_2^{2-}) as substrates, in contrast to the substrates utilized by canonical 2,3-catechol dioxygenase. Structural analysis of ChaP and its homologues ChaP-H1 and ChaP-H2 indicated that the overall structures of these dimeric proteins are similar to those of 2,3-catechol dioxygenase despite lacking sequence similarity. Docking studies and site-directed mutagenesis analysis of ChaP provided mechanistic insight into the unusual oxidative rearrangement. This novel strategy for the construction of the pharmaceutically important α-pyrone ring can be applied to the development of diverse antibiotic derivatives with potent biological activities. Our study resolves the long-standing mystery in chartreusin biosynthesis[6,7,21] and expands the catalytic diversity of the VOC enzyme superfamily.

ASSOCIATED CONTENT

Supporting Information

The Supporting Information is available free of charge on the ACS Publications website at DOI: 10.1021/jacs.8b06623.

Experimental procedures and spectroscopic data, including Tables S1–S23 and Figures S1–S70 (PDF)
Jmol molecular structure file for ChaP (PDB)
Jmol molecular structure file for ChaP-H1 (PDB)
Jmol molecular structure file for ChaP-H2 (PDB)

AUTHOR INFORMATION

Corresponding Authors

*zhujiapeng@hotmail.com
*rxtan@nju.edu.cn
*hmge@nju.edu.cn

ORCID

Fang Liu: 0000-0002-0046-8434

DOI: 10.1021/jacs.8b06623
J. Am. Chem. Soc. 2018, 140, 10909–10914

Suwen Zhao: 0000-0001-5609-434X
Yong Liang: 0000-0001-5026-6710
Ren Xiang Tan: 0000-0001-6532-6261
Hui Ming Ge: 0000-0002-0468-808X

Author Contributions

[Δ]Y.S.W. and B. Z. contributed equally.

Notes

The authors declare no competing financial interest.

■ ACKNOWLEDGMENTS

The authors thank Drs. Jeffrey D. Rudolf (Scripps Research Institute), Zhengren Xu (Peking University), and Huan Wang (Nanjing University) for critical reading and helpful discussion. This work was financially supported by the Natural Science Foundation of China (Nos. 21572100, 81522042, 81773591, 81421091, 81500059, 81673333, 21672101, 21761142001, and 21661140001), Fundamental Research Funds for the Central Universities (no. 020814380092), ShanghaiTech University, and Jiangsu Specially Appointed Professor Funding.

■ REFERENCES

(1) Kong, L.; Zhang, W.; Chooi, Y. H.; Wang, L.; Cao, B.; Deng, Z.; Chu, Y.; You, D. *Cell Chem. Biol.* **2016**, *23*, 508.
(2) Fan, K.; Pan, G.; Peng, X.; Zheng, J.; Gao, W.; Wang, J.; Wang, W.; Li, Y.; Yang, K. *Chem. Biol.* **2012**, *19*, 1381.
(3) Wendt-Pienkowski, E.; Huang, Y.; Zhang, J.; Li, B. S.; Jiang, H.; Kwon, H. J.; Hutchinson, C. R.; Shen, B. *J. Am. Chem. Soc.* **2005**, *127*, 16442.
(4) Yunt, Z.; Reinhardt, K.; Li, A.; Engeser, M.; Dahse, H. M.; Gutschow, M.; Bruhn, T.; Bringmann, G.; Piel, J. *J. Am. Chem. Soc.* **2009**, *131*, 2297.
(5) Wang, B.; Ren, J.; Li, L.; Guo, F.; Pan, G.; Ai, G.; Aigle, B.; Fan, K.; Yang, K. *Chem. Commun.* **2015**, *51*, 8845.
(6) Xu, Z. G.; Jakobi, K.; Welzel, K.; Hertweck, C. *Chem. Biol.* **2005**, *12*, 579.
(7) Tang, M.-C.; Zou, Y.; Watanabe, K.; Walsh, C. T.; Tang, Y. *Chem. Rev.* **2017**, *117*, 5226.
(8) Leach, B. E.; Calhoun, K. M.; Johnson, L. E.; Teeters, C. M.; Jackson, W. G. *J. Am. Chem. Soc.* **1953**, *75*, 4011.
(9) Ueberschaar, N.; Xu, Z. L.; Scherlach, K.; Metsa-Ketela, M.; Bretschneider, T.; Dahse, H. M.; Gorls, H.; Hertweck, C. *J. Am. Chem. Soc.* **2013**, *135*, 17408.
(10) Aoyama, Y.; Katayama, T.; Yamamoto, M.; Tanaka, H.; Kon, K. *J. Antibiot.* **1992**, *45*, 875.
(11) Takai, M.; Uehara, Y.; Beisler, J. A. *J. Med. Chem.* **1980**, *23*, 549.
(12) Yang, C.-L.; Wang, Y.-S.; Liu, C.-L.; Zeng, Y.-J.; Cheng, P.; Jiao, R.-H.; Bao, S.-X.; Huang, H.-Q.; Tan, R.-X.; Ge, H.-M. *Mar. Drugs* **2017**, *15*, 244.
(13) He, P. Q.; Moran, G. R. *J. Inorg. Biochem.* **2011**, *105*, 1259.
(14) Mendel, S.; Arndt, A.; Bugg, T. D. H. *Biochemistry* **2004**, *43*, 13390.
(15) Sanvoisin, J.; Langley, G. J.; Bugg, T. D. H. *J. Am. Chem. Soc.* **1995**, *117*, 7836.
(16) Walsh, C. T.; Wencewicz, T. A. *Nat. Prod. Rep.* **2013**, *30*, 175.
(17) Lin, S.; Van Lanen, S. G.; Shen, B. *J. Am. Chem. Soc.* **2008**, *130*, 6616.
(18) Holm, L.; Rosenstrom, P. *Nucleic Acids Res.* **2010**, *38*, W545.
(19) Sato, N.; Uragami, Y.; Nishizaki, T.; Takahashi, Y.; Sazaki, G.; Sugimoto, K.; Nonaka, T.; Masai, E.; Fukuda, M.; Senda, T. *J. Mol. Biol.* **2002**, *321*, 621.
(20) Farid, R.; Day, T.; Friesner, R. A.; Pearlstein, R. A. *Bioorg. Med. Chem.* **2006**, *14*, 3160.
(21) Gao, S. S.; Zhang, T.; Garcia-Borras, M.; Hung, Y. S.; Billingsley, J. M.; Houk, K. N.; Hu, Y.; Tang, Y. *J. Am. Chem. Soc.* **2018**, *140*, 6991.

■ NOTE ADDED AFTER ASAP PUBLICATION

This paper posted on August 15, 2017. Panel G of Figure 3 was missing. This has been corrected and the paper was re-posted on August 16, 2018.

DOI: 10.1021/jacs.8b06623
J. Am. Chem. Soc. 2018, 140, 10909−10914